dilution heats, calorimetric data was analysed using the evaluation software MicroCal Origin v5.0 (MicroCal Software). Negative binding results from ITC (for Arf·GDP, Rho·GDP/GTP and Cdc42·GDP/GTP) were confirmed by either fluorescence anisotropy (using mant-nucleotide), surface plasmon resonance, or both.

Fluorescence anisotropy titrations

Competition experiments were performed using an ISS PC1 spectrofluorimeter. All measurements were taken at 20° C with $\lambda_{ex} = 366$ nm. We viewed emission through a KV399 cutoff filter, and recorded the measurements using the L format of the instrument. Rac1 was loaded with either mant-GDP or mant-GMPPNP, and mixed with stoichiometric amounts of Araptin (dimer). The mixture was placed in the cuvette and titrated against either Arf1·GDP, Arf1·GMPPNP, Rac1·GDP or Rac1·GMPPNP while the change in fluorescence anisotropy was monitored.

1. Macara, I. G., Lounsbury, K. M., Richards, S. A., McKiernan, C. & Bar-Sagi, D. The Ras superfamily of GTPases. *FASEB J.* **10**, 625–630 (1996).
2. Bar-Sagi, D. & Hall, A. Ras and Rho GTPases: A family reunion. *Cell* **103**, 227–238 (2000).
3. Fensome, A., Whatmore, J., Morgan, C., Jones, D. & Cockcroft, S. ADP-ribosylation factor and Rho proteins mediate fMLP-dependent activation of phospholipase D in human neutrophils. *J. Biol. Chem.* **273**, 13157–13164 (1998).
4. Zhang, Q., Calafat, J., Janssen, H. & Greenberg, S. ARF6 is required for growth factor- and rac-mediated membrane ruffling in macrophages at a stage distal to rac membrane targeting. *Mol. Cell. Biol.* **19**, 8158–8168 (1999).
5. Wu, W. J., Erickson, J. W., Lin, R. & Cerione, R. A. The γ-subunit of the coatomer complex binds Cdc42 to mediate transformation. *Nature* **405**, 800–804 (2000).
6. Walker, S. J., Wu, W. J., Cerione, R. A. & Brown, H. A. Activation of phospholipase D1 by Cdc42 requires the Rho insert region. *J. Biol. Chem.* **275**, 15665–15668 (2000).
7. Boshans, R. L., Szanto, S., van Aelst, L. & D'Souza-Schorey, C. ADP-ribosylation factor 6 regulates actin cytoskeleton remodeling in coordination with Rac1 and RhoA. *Mol. Cell. Biol.* **20**, 3685–3694 (2000).
8. D'Souza-Schorey, C., Boshans, R. L., McDonough, M., Stahl, P. D. & Van Aelst, L. A role for POR1, a Rac1-interacting protein, in ARF6-mediated cytoskeletal rearrangements. *EMBO J.* **16**, 5445–5454 (1997).
9. Van Aelst, L., Joneson, T. & Bar-Sagi, D. Identification of a novel Rac1-interacting protein involved in membrane ruffling. *EMBO J.* **15**, 3778–3786 (1996).
10. Kanoh, H., Williger, B. T. & Exton, J. H. Arfaptin 1, a putative cytosolic target protein of ADP-ribosylation factor, is recruited to Golgi membranes. *J. Biol. Chem.* **272**, 5421–5429 (1997).
11. Williger, B. T., Ostermann, J. & Exton, J. H. Arfaptin 1, an ARF-binding protein, inhibits phospholipase D and endoplasmic reticulum/Golgi protein transport. *FEBS Lett.* **443**, 197–200 (1999).
12. Joneson, T., McDonough, M., Bar-Sagi, D. & Van Aelst, L. RAC regulation of actin polymerization and proliferation by a pathway distinct from Jun kinase. *Science* **274**, 1374–1376 (1996).
13. Maesaki, R. *et al.* The structural basis of Rho effector recognition revealed by the crystal structure of human RhoA complexed with the effector domain of PKN/PRK1. *Mol. Cell* **4**, 793–803 (1999).
14. Lapouge, K. *et al.* Structure of the TPR domain of p67phox in complex with Rac·GTP. *Mol. Cell* **6**, 1–20 (2000).
15. Geyer, M. & Wittinghofer, A. GEFs, GAPs, GDIs and effectors: taking a closer (3D) look at the regulation of Ras-related GTP-binding proteins. *Curr. Opin. Struct. Biol.* **7**, 786–792 (1997).
16. Hoffman, G. R., Nassar, N. & Cerione, R. A. Structure of the Rho family GTP-binding protein Cdc42 in complex with the multifunctional regulator RhoGDI. *Cell* **100**, 345–356 (2000).
17. Scheffzek, K., Stephan, I., Jensen, O. N., Illenberger, D. & Gierschik, P. The Rac–RhoGDI complex and the structural basis for the regulation of Rho proteins by RhoGDI. *Nature Struct. Biol.* **7**, 122–126 (2000).
18. Wittinghofer, A. Signal transduction via Ras. *Biol. Chem.* **379**, 933–937 (1998).
19. Pacold, M. E. *et al.* Crystal structure and functional analysis of ras binding to its effector phosphoinositide 3-kinase γ. *Cell* **103**, 931–943 (2000).
20. Franco, M. *et al.* EFA6, a sec7 domain-containing exchange factor for ARF6, coordinates membrane recycling and actin cytoskeleton organization. *EMBO J.* **18**, 1480–1491 (1999).
21. Otwinowski, Z. & Minor, W. in *Data Collection and Processing* (eds Sawyer, L., Isaacs, N. & Bailey, S.) 556–562 (Daresbury Laboratory, Warrington, UK, 1993).
22. Terwilliger, T. C. & Berendzen, J. Automated MAD and MIR structure solution. *Acta Crystallogr. D* **55**, 849–861 (1999).
23. Jones, T. A., Zhou, J. Y., Cowan, S. W. & Kjeldgaard, M. Improved methods for building protein models in electron density maps and the location of errors in these models. *Acta Crystallogr. A* **47**, 110–119 (1991).
24. Collaborative Computer Project No. 4. The CCP4 suite: programs for protein crystallography. *Acta Crystallogr. D* **50**, 760–763 (1994).
25. Brunger, A. T. *et al.* Crystallography & NMR system: A new software suite for macromolecular structure determination. *Acta Crystallogr. D* **54**, 905–921 (1998).
26. Kraulis, P. J. MOLSCRIPT: A program to produce both detailed and schematic plots of protein structures. *J. Appl. Crystallogr.* **24**, 946–950 (1991).

....

errata

Drought-induced guard cell signal transduction involves sphingosine-1-phosphate

Carl K.-Y. Ng, Kathryn Carr, Martin R. McAinsh, Brian Powell & Alistair M. Hetherington

Nature **410**, 596–599 (2001).

....

In the second paragraph of this paper, (*trans*-4-sphingenine, d18:1 (ref. 4)) should have read (*trans*-4-sphingenine, d18:1[4]); (d18:1 (ref. 8)) should have read (d18:1[8]); (d18:2 (refs 4,8)) should have read (d18:2[4,8]); and (t18:1 (ref. 10)) should have read (t18:1[8])[10]. □

BRI1 is a critical component of a plasma-membrane receptor for plant steroids

Zhi-Yong Wang, Hideharu Seto, Shozo Fujioka, Shigeo Yoshida & Joanne Chory

Nature **410**, 380–383 (2001).

....

In Figure 3b, the label for CIP at the third lane should be + rather than −. □

letters to nature

the molecular mechanisms of cardiac excitation–contraction coupling, and may have important implications for studying Ca^{2+} signalling in general. ☐

Methods

Confocal Ca^{2+} imaging

Enzymatically isolated adult rat ventricular myocytes were loaded with the Ca^{2+} indicator fluo-4-AM as described[6,28]. Confocal line-scan imaging was performed using a Zeiss LSM 410 or LSM510 confocal microscope equipped with an argon laser (488 nm) and a ×40, 1.3NA oil immersion objective. Line-scan images were acquired at sampling rates of 0.7 or 1.4 ms per line and 0.07 μm per pixel, with radial and axial resolutions of 0.4 and 1.0 μm, respectively. Digital image analysis was performed using IDL software (Research Systems) and customer-devised routines[6,22]. In SR-paralysed cells, local Ca^{2+} transients were indexed by the normalized local fluorescence, F/F_0 (F_0 refers to the level before depolarization). In cells with intact SR function, local Ca^{2+} transients were determined using the following formula[6]:

$$[Ca^{2+}] = k_d R/(k_d/[Ca^{2+}]_{rest} + 1 - R)$$

where $R = F/F_0$, the resting Ca^{2+} concentration $[Ca^{2+}]_{rest} = 100$ nM, and the dissociation constant $k_d = 1.1$ μM (in accordance with the value for fluo-3 in cells[29]).

Cell-attached patch clamp

Cell-attached patch clamps were established in either GΩ-seal or loose-seal configuration[7], with glass patch pipettes of 5–7 MΩ. In GΩ-seal patches, unitary Ca^{2+} currents were recorded by using a cooled capacitor feedback headstage (CV203B) and an Axopatch 200 B amplifier (Axon Instruments). Current records were low-pass filtered at 1 kHz, digitized at 5 kHz, and are presented with leak and capacity currents eliminated by subtraction of smooth functions, as described[9]. For loose-seal patch clamp experiments, membrane potential was determined by proportionally dividing the test voltages between the pipette resistance (5–7 MΩ) and the seal resistance (20–50 MΩ). The surface-charge shielding effect by high Ca^{2+} or Ba^{2+} was not corrected.

Solutions

The standard patch pipette filling solution contained (in mM): 120 tetraethylammonium chloride, 20 $CaCl_2$, 0.01 tetrodotoxin, 0.01 FPL64176 and 10 HEPES, pH 7.4, unless specified otherwise. In experiments shown in Fig. 1, the extracellular solution outside the patch membrane contained (in mM): 100 potassium aspartate, 40 KCl, 10 HEPES, 1 EGTA, 5 Mg^{2+}-ATP, 10 caffeine and 0.01 thapsigargin, pH 7.3. In other experiments, the standard superfusion solution contained (in mM): 135 NaCl, 1 $CaCl_2$, 4 KCl, 1 $MgCl_2$, 10 glucose, 10 HEPES, pH 7.4 . All experiments were performed at room temperature (23–25 °C).

Statistics

Data were expressed as mean ± s.e.m. Student's t-test, paired t-test and χ^2-test were applied when appropriate. A P value less than 0.05 was considered statistically significant.

1. Hong, K., Nishiyama, M., Henley, J., Tessier-Lavigne, M. & Poo, M.-M. Calcium signalling in the guidance of nerve growth by netrin-1. *Nature* **403**, 93–98 (2000).
2. Clapham, D. E. Calcium signaling. *Cell* **80**, 259–268 (1995).
3. Berridge, M. J. Inositol trisphosphate and calcium signalling. *Nature* **361**, 315–325 (1993).
4. Bers, D. M. & Perez-Reyes, E. Ca channels in cardiac myocytes: structure and function in Ca influx and intracellular Ca release. *Cardiovasc. Res.* **42**, 339–360 (1999).
5. Fabiato, A. Time and calcium dependence of activation and inactivation of calcium-induced release of calcium from the sarcoplasmic reticulum of a skinned canine cardiac Purkinje cell. *J. Gen. Physiol.* **85**, 247–289 (1985).
6. Cheng, H., Lederer, W. J. & Cannell, M. B. Calcium sparks: elementary events underlying excitation-contraction coupling in heart muscle. *Science* **262**, 740–744 (1993).
7. Hamill, O. P., Marty, A., Neher, E., Sakmann, B. & Sigworth, F. J. Improved patch-clamp techniques for high-resolution current recording from cells and cell-free membrane patches. *Pflugers Arch.* **391**, 85–100 (1981).
8. Kunze, D. L. & Rampe, D. Characterization of the effects of a new Ca^{2+} channel activator, FPL 64176, in GH3 cells. *Mol. Pharmacol.* **42**, 666–670 (1992).
9. Sham, J. S. et al. Termination of Ca^{2+} release by a local inactivation of ryanodine receptors in cardiac myocytes. *Proc. Natl Acad. Sci. USA* **95**, 15096–15101 (1998).
10. Franzini-Armstrong, C., Protasi, F. & Ramesh, V. Shape, size, and distribution of Ca^{2+} release units and couplons in skeletal and cardiac muscles. *Biophys. J.* **77**, 1528–1539 (1999).
11. Carl, S. L. et al. Immunolocalization of sarcolemmal dihydropyridine receptor and sarcoplasmic reticular triadin and ryanodine receptor in rabbit ventricle and atrium. *J. Cell. Biol.* **129**, 672–682 (1995).
12. Stern, M. D. Theory of excitation-contraction coupling in cardiac muscle. *Biophys. J.* **63**, 497–517 (1992).
13. Niggli, E. & Lederer, W. J. Voltage-independent calcium release in heart muscle. *Science* **250**, 565–568 (1990).
14. Cannell, M. B., Cheng, H. & Lederer, W. J. The control of calcium release in heart muscle. *Science* **268**, 1045–1049 (1995).
15. López-López, J. R., Shacklock, P. S., Balke, C. W. & Wier, W. G. Local calcium transients triggered by single L-type calcium channel currents in cardiac cells. *Science* **268**, 1042–1045 (1995).
16. Shorofsky, S. R., Izu, L., Wier, W. G. & Balke, C. W. Ca^{2+} sparks triggered by patch depolarization in rat heart cells. *Circ. Res.* **82**, 424–429 (1998).
17. Santana, L. F., Cheng, H., Gómez, A. M., Cannell, M. B. & Lederer, W. J. Relation between the sarcolemmal Ca^{2+} current and Ca^{2+} sparks and local control theories for cardiac excitation-contraction coupling. *Circ. Res.* **78**, 166–171 (1996).
18. Soeller, C. & Cannell, M. B. Numerical simulation of local calcium movements during L-type calcium channel gating in the cardiac diad. *Biophys. J.* **73**, 97–111 (1997).
19. Györke, S. & Fill, M. Ryanodine receptor adaptation: control mechanism of Ca^{2+}-induced Ca^{2+} release in heart. *Science* **260**, 807–809 (1993).
20. Lipp, P. & Niggli, E. Fundamental calcium release events revealed by two-photon excitation photolysis of caged calcium in guinea-pig cardiac myocytes. *J. Physiol. (Lond.)* **508**, 801–809 (1998).
21. Bridge, J. H., Ershler, P. R. & Cannell, M. B. Properties of Ca^{2+} sparks evoked by action potentials in mouse ventricular myocytes. *J. Physiol. (Lond.)* **518**, 469–478 (1999).
22. Cheng, H. et al. Amplitude distribution of calcium sparks in confocal images: theory and studies with an automatic detection method. *Biophys. J.* **76**, 606–617 (1999).
23. González, A. et al. Involvement of multiple intracellular release channels in calcium sparks of skeletal muscle. *Proc. Natl Acad. Sci. USA* **97**, 4380–4385 (2000).
24. Schneider, M. F. Ca^{2+} sparks in frog skeletal muscle: generation by one, some, or many SR Ca^{2+} release channels? *J. Gen. Physiol.* **113**, 365–372 (1999).
25. Bootman, M. D. & Berridge, M. J. The elemental principles of calcium signaling. *Cell* **83**, 675–678 (1995).
26. Blatter, L. A., Hüser, J. & Ríos, E. Sarcoplasmic reticulum Ca^{2+} release flux underlying Ca^{2+} sparks in cardiac muscle. *Proc. Natl Acad. Sci. USA* **94**, 4176–4181 (1997).
27. Mejía-Alvarez, R., Kettlun, C., Ríos, E., Stern, M. & Fill, M. Unitary Ca^{2+} current through cardiac ryanodine receptor channels under quasi-physiological ionic conditions. *J. Gen. Physiol.* **113**, 177–186 (1999).
28. Xiao, R. P., Spurgeon, H. A., O'Connor, F. & Lakatta, E. G. Age-associated changes in beta-adrenergic modulation on rat cardiac excitation-contraction coupling. *J. Clin. Invest.* **94**, 2051–2059 (1994).
29. Harkins, A. B., Kurebayashi, N. & Baylor, S. M. Resting myoplasmic free calcium in frog skeletal muscle fibers estimated with fluo-3. *Biophys. J.* **65**, 865–881 (1993).

··

Drought-induced guard cell signal transduction involves sphingosine-1-phosphate

Carl K.-Y. Ng, Kathryn Carr†, Martin R. McAinsh**, Brian Powell†
& Alistair M. Hetherington**

* Department of Biological Sciences, Institute of Environmental and Natural Sciences, Lancaster University, Bailrigg, Lancaster LA1 4YQ, UK
† Avecia Limited, Hexagon House, Blackley, Manchester M9 8ZS, UK

....

Stomata form pores on leaf surfaces that regulate the uptake of CO_2 for photosynthesis and the loss of water vapour during transpiration[1]. An increase in the cytosolic concentration of free calcium ions ($[Ca^{2+}]_{cyt}$) is a common intermediate in many of the pathways leading to either opening or closure of the stomatal pore[2,3]. This observation has prompted investigations into how specificity is controlled in calcium-based signalling systems in plants. One possible explanation is that each stimulus generates a unique increase in $[Ca^{2+}]_{cyt}$, or 'calcium signature', that dictates the outcome of the final response[4]. It has been suggested that the key to generating a calcium signature, and hence to understanding how specificity is controlled, is the ability to access differentially the cellular machinery controlling calcium influx and release from internal stores[2–5]. Here we report that sphingosine-1-phosphate is a new calcium-mobilizing molecule in plants. We show that after drought treatment sphingosine-1-phosphate levels increase, and we present evidence that this molecule is

involved in the signal-transduction pathway linking the perception of abscisic acid to reductions in guard cell turgor.

In animal cells, sphingosine-1-phosphate (S1P) has been reported to be involved in the mediation of numerous cellular responses including proliferation, survival, cytoskeletal organization, motility, differentiation and neurite retraction and rounding[6–8]. As a first step to establishing whether S1P is an endogenous calcium-mobilizing compound in plants, we confirmed its presence in plant extracts. In animals, the predominant sphingoid base is sphingosine (*trans*-4-sphingenine, d18:1 (ref. 4)) with lesser amounts of sphinganine (d18:0) and 4-hydroxysphinganine (t18:0)[9]. In contrast, sphingoid bases from plants are predominantly sphinganine, 4-hydroxysphinganine and *cis* and *trans* isomers of 8-sphingenine (d18:1 (ref. 8)), 4,8-sphingadiene (d18:2 (refs 4, 8)) and 4-hydroxy-8-sphingenine (t18:1 (ref. 10)). (Note that d and t denote a dihydroxy and trihydroxy base, respectively.)

We extracted lipids from mature, fully expanded leaves of *Commelina communis*. The lipid extract was fractionated by high-performance liquid chromatography (LC) and the fraction corresponding to S1P was eluted. The putative S1P fraction was subjected to tandem mass spectrometry (MS/MS) in both positive and negative ionization modes and the corresponding product ion spectra were compared with those obtained using authentic S1P. The positive-ion LC/MS/MS product ion spectrum of m/z 380 $(M+H)^+$ from the lipid extract (Fig. 1a) matched the spectrum obtained from authentic S1P (Fig. 1b). The negative-ion LC/MS/MS product ion spectrum of m/z 378 $(M-H)^-$ from the lipid extract showed a single peak at m/z 79 corresponding to the phosphoryl group, matching that obtained from authentic S1P (data not shown). The results of this experiment confirmed the presence of S1P in plants. Notably, our results also challenge the current consensus that plants are devoid of sphingoid bases with the Δ4-double bond[10]. We estimate that the levels of S1P in leaves range from 5 to 46 pg per g dry weight (on the basis of a recovery of ~16%). In addition, when plants were subject to drought treatments, we observed a 1.3–2.4-fold increase in S1P compared with levels in well-watered controls in four out of six pairwise comparisons (see Supplementary Information Table 1). Although the conditions for S1P extraction have yet to be fully optimized for plant tissue, these data suggest that decreased water availability might be associated with increased S1P levels in leaves.

We next tested the ability of S1P to modulate guard cell turgor by measuring changes in stomatal apertures after incubation of epidermal strips of *C. communis* in buffer containing S1P. S1P (4–6 μM) promoted the closure of opened stomata (Fig. 2a). The effect of S1P is reversible, as determined by wash-out experiments, indicating that the observed effect was not due to irreversible cytotoxicity. In addition, guard cells treated with S1P were morphologically normal and showed a normal pattern of organelle distribution, providing further evidence that the effect of S1P was not due to cytotoxicity (data not shown). Studies using animal cells showed that the presence of the Δ4-double bond is essential for S1P to mediate its intracellular effects[11]. To test whether the effect of S1P is specific and dependent on the Δ4-double bond, we used the structurally similar sphingoid base, dihydro-S1P, which is derived from S1P by hydrogenation of the Δ4-double bond. Dihydro-S1P did not affect stomatal apertures (Fig. 2b), providing evidence that the effect of S1P is specific and dependent on the presence of the Δ4-double bond. Our results also indicate that dihydro-S1P can function as an inactive analogue in stomatal guard cells, an observation in good agreement with results obtained from animal cell studies[11].

In animal cells, the effect of S1P on cellular function is calcium dependent[6–8]. As inclusion of 2 mM EGTA resulted in complete abolition of the effect of S1P on stomatal aperture, the same relationship holds in guard cells (Fig. 2c). To investigate the involvement of calcium directly, we pressure-microinjected the Ca^{2+}-sensitive fluorescent indicator, Fura-2, into the cytosol of single guard cells and measured changes in $[Ca^{2+}]_{cyt}$ in response to 6 μM ($n = 4$) and 50 μM ($n = 6$) S1P. The resting levels of $[Ca^{2+}]_{cyt}$ in these cells ($n = 10$) were 50–120 nM. When challenged with 6 μM S1P, oscillations in $[Ca^{2+}]_{cyt}$ were observed. The oscillations induced by 6 μM S1P were rapid and asymmetrical, with a period of 3.8 ± 0.4 min ($n = 4$) (Fig. 3a). The elevations in $[Ca^{2+}]_{cyt}$
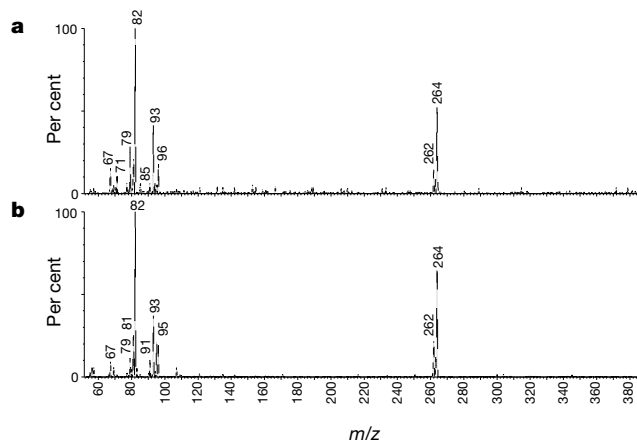
Figure 1 Positive-ion LC/MS/MS product ion spectra of m/z 380 $(M+H)^+$. **a**, Product ion spectrum from a partially purified lipid extract of mature, fully expanded leaves of *C. communis* (see Methods). **b**, Product ion spectrum from authentic S1P.
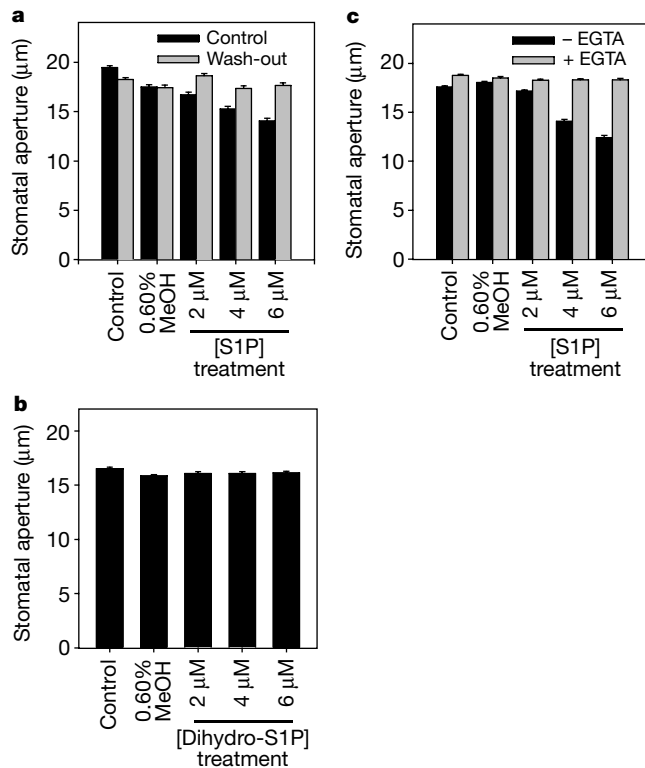
Figure 2 Effects of S1P and dihydro-S1P on stomatal aperture. **a**, Apertures of opened stomata after a 2-h incubation in S1P (black columns) and a subsequent 2-h wash-out (grey columns). **b**, Apertures of opened stomata after a 2-h incubation in dihydro-S1P. **c**, Apertures of opened stomata after a 2-h incubation in S1P (black bars) and S1P + 2 mM EGTA (grey columns). Values are means ± s.e.m. ($n = 180$).

ranged from 30 to 50 nM above resting levels. Rapid and symmetrical oscillations in $[Ca^{2+}]_{cyt}$ with a period of 2.8 ± 0.2 min were observed ($n = 6$) when guard cells were challenged with 50 μM S1P (Fig. 3b). The elevations in $[Ca^{2+}]_{cyt}$ induced by 50 μM S1P were 50–100 nM above resting levels. Although elevation in $[Ca^{2+}]_{cyt}$ is an integral downstream effect of S1P in all animal cell types examined[6–8], our data represent the first report of S1P-induced $[Ca^{2+}]_{cyt}$ oscillations. Challenging guard cells with S1P induced $[Ca^{2+}]_{cyt}$ oscillations in every experiment we performed.

To determine whether the effect of S1P on guard cell $[Ca^{2+}]_{cyt}$ is specific, we challenged single guard cells, pressure-microinjected with Fura-2 ($n = 5$) with 50 μM dihydro-S1P and measured $[Ca^{2+}]_{cyt}$. Resting levels of $[Ca^{2+}]_{cyt}$ in these cells were 80–120 nM, and when challenged with dihydro-S1P no change in $[Ca^{2+}]_{cyt}$ was observed ($n = 5$). When these same cells were subsequently challenged with 1 mM Ca^{2+}, a characteristic pattern of $[Ca^{2+}]_{cyt}$ oscillations[12] was observed, demonstrating that these cells possessed functional calcium homeostatic machinery (Fig. 3c). These results show that, like other signals[13–16], S1P induces closure of the stomatal pore by generating an increase in $[Ca^{2+}]_{cyt}$. In the case of S1P the increases take the form of oscillations in $[Ca^{2+}]_{cyt}$, which have a period and amplitude characteristic of the concentration of S1P used. There was a lag period of about 120 and 4 min after the initiation of the oscillations in response to 6 μM (Fig. 3d) and 50 μM (Fig. 3e) S1P, respectively, before changes in stomatal apertures were observed. These data point towards a physiological role for oscillations in $[Ca^{2+}]_{cyt}$ induced by S1P in mediating changes in guard cell turgor.

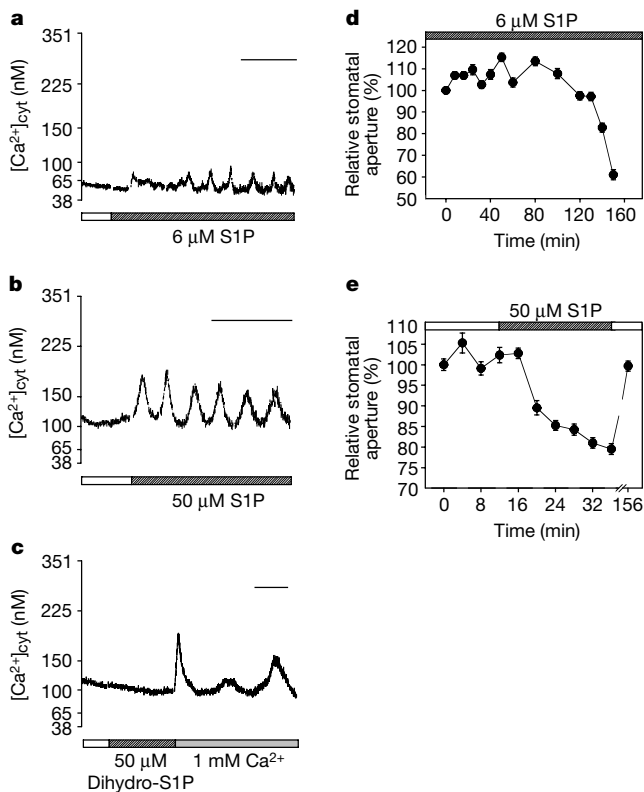**Figure 3** Effects of S1P and dihydro-S1P on guard cell $[Ca^{2+}]_{cyt}$, and kinetics of S1P-induced stomatal closure. **a**, Representative trace ($n = 4$) of oscillations in guard cell $[Ca^{2+}]_{cyt}$ induced by 6 μM S1P. **b**, Representative trace ($n = 6$) of oscillations in $[Ca^{2+}]_{cyt}$ induced by 50 μM S1P. **c**, Representative trace ($n = 5$) showing the inability of 50 μM dihydro-S1P to induce a change in $[Ca^{2+}]_{cyt}$. Time bar, 10 min. In **d** and **e** stomata were pre-opened in KCl-MES buffer for 3 h before transfer to KCl-MES buffer containing S1P. **d**, Rates of stomatal closure in response to 6 μM S1P. **e**, Rates of stomatal closure in response to 50 μM S1P. Values are means $\pm$ s.e.m. ($n = 40$).
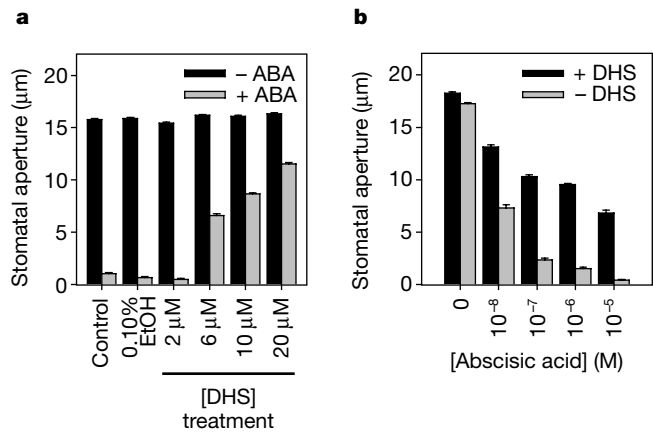

Figure 4 Effect of DHS on ABA-induced stomatal closure. **a**, Stomatal apertures after a 3-h pretreatment in buffer containing various concentrations of DHS (black columns), and 2 h after transfer to buffer containing 100 nM ABA (grey columns). **b**, Epidermal strips were pretreated with buffer only (grey columns) or buffer containing 20 μM DHS (black columns) for 3 h and apertures of opened stomata were measured after a subsequent 2-h incubation in buffer containing various concentrations of ABA. Values are means $\pm$ s.e.m. ($n = 180$).

As the regulation of stomatal turgor by abscisic acid (ABA) involves an increase in $[Ca^{2+}]_{cyt}$ (refs 17, 18), we next investigated whether S1P is a component of the guard cell ABA signalling pathway. We used DL-threo-dihydrosphingosine (DHS), which in animal cells is a competitive inhibitor of sphingosine kinase[19,20], to decrease cellular S1P levels. On its own, DHS did not affect stomatal apertures. However, in epidermal strips that had been pretreated with DHS, the effect of ABA on stomatal closure was attenuated. The attenuation of the ABA response was partial and dose dependent (Fig. 4a). In another experiment, we tested the ability of DHS to attenuate the effect of various concentrations of ABA ranging from 10^{-8} M to 10^{-5} M. Attenuation of the effect of ABA is partial, regardless of the concentration of ABA used (Fig. 4b). This is in agreement with the current understanding of an inherent redundancy in the ABA signal-transduction pathway regulating guard cell turgor[5].

In summary, we have provided a positive identification of sphingosine-1-phosphate in plants. We also present evidence that the levels of S1P increase in leaves after drought and that S1P is a calcium-mobilizing compound active in the signal-transduction pathway linking ABA to reductions in stomatal aperture. Our data also suggest that the messenger role of S1P is evolutionarily conserved between animals and plants. □

Methods

Stomatal bioassay and $[Ca^{2+}]_{cyt}$ measurements

Commelina communis L. plants were grown from seed at 20–25 °C, and stomatal aperture bioassays using isolated abaxial epidermal peels were conducted as described[15–17]. We measured guard cell $[Ca^{2+}]_{cyt}$ as described[12].

Lipid extraction and analysis

Lipid was extracted from mature, fully expanded leaves. Freshly harvested leaves (20 g) were homogenized with liquid N_2. The homogenate was extracted with 100 ml of ice-cold 1:2 chloroform:methanol (v/v) for 45 min under constant agitation and filtered. We added 48 ml of chloroform, 48 ml of 1 M KCl and 2 ml of 10% NH_4OH to the filtrate and mixed it thoroughly. Phases were separated by centrifugation and the upper alkaline phase was retained, to which 80 ml of chloroform and 4 ml of concentrated HCl were added. The sample was mixed thoroughly, and the phases were separated by centrifugation. The resultant upper phase was discarded, and the lower chloroform phase was retained. The chloroform was evaporated to dryness, and the sample was kept at -20 °C for analysis.

The extracted lipids were analysed by atmospheric pressure ionization (API) liquid chromatography (LC) tandem mass spectrometry (MS/MS). Both LC/MS and LC/MS/MS experiments were performed on a HP1050 liquid chromatograph with a quaternary solvent delivery system, coupled to a SCIEX (Thornhill, Ontario, Canada) API III+ triple quadrupole mass spectrometer equipped with an API source, through an IonSpray (ISP) interface. High-purity nitrogen was used as the curtain gas in the API source at a flow rate

of $0.8\,l\,min^{-1}$. LC conditions were Vydac C_4 protein HPLC column (15 cm × 4.6 mm i.d.) using an acetonitrile:water:tetrahydrofuran gradient at $1\,ml\,min^{-1}$. For this interface, the column effluent was split using a zero-dead-volume T connector, with a split ratio of 25:1 determined by the length of a fused silica capillary on the waste side of the T. The remainder of the column effluent was fed to the transfer line of the interface. The ISP needle was maintained at 5.5 kV. High-purity nitrogen was used as the nebulizing gas at a flow rate of $0.6\,l\,min^{-1}$. A Macintosh Quadra900 computer was used for instrument control, data acquisition and data processing. A dwell time of 10 ms Da^{-1} was used for full-scan (m/z 50–400) LC/MS analyses.

MS/MS measurements were based on collision-induced dissociations (CID) within the radiofrequency-only quadrupole at a collision energy of 30 eV. Argon was used as the collision gas at an indicated thickness of 220. Extraction efficiency was obtained from replicate spiking experiments and was determined ∼16%.

For drought experiments, water was withheld for a total of 11 days. Leaves were harvested at the end of the 11-day drought period. Parallel control samples were harvested from well-watered plants. A 11-day drought period resulted in a significant reduction in the fresh weight/dry weight ratio compared with well-watered controls ($P < 0.001$, t test). Lipids were extracted from leaf samples from well-watered plants and plants subjected to a drought treatment. S1P levels were quantified by LC/MS as described above. Estimation of S1P levels in the lipid extracts was based on a linear calibration ($r^2 = 0.996$) obtained from areas under peaks of LC/MS analysis of known concentrations of authentic S1P. S1P levels are expressed in terms of dry weight of leaves based on linear calibrations of fresh weight versus dry weight from well-watered control plants ($r^2 = 1.000$) and plants subjected to the drought treatment ($r^2 = 0.999$).

Preparation of sphingolipid solutions

S1P, dihydro-S1P and DHS were obtained from Biomol (Plymouth Meeting, Pennsylvania, USA) and stock solutions were prepared in methanol (S1P and dihydro-S1P) or ethanol (DHS).

1. Willmer, C. & Fricker, M. *Stomata* 2nd edn (Chapman & Hall, London, 1996).
2. MacRobbie, E. A. C. Signal transduction and ion channels in guard cells. *Phil. Trans. R. Soc. Lond. B* **353**, 1475–1488 (1998).
3. Sanders, D., Brownlee, C. & Harper, J. F. Communicating with calcium. *Plant Cell* **11**, 691–706 (1999).
4. McAinsh, M. R. & Hetherington, A. M. Encoding specificity in Ca^{2+} signalling systems. *Trends Plant Sci.* **3**, 32–36 (1998).
5. Blatt, M. R. Ca^{2+} signalling and control of guard-cell volume in stomatal movements. *Curr. Opin. Plant Biol.* **3**, 196–204 (2000).
6. Mattie, M. E., Brooker, G. & Spiegel, S. Sphingosine-1-phosphate, a putative second messenger, mobilizes calcium from internal stores via an inositol trisphosphate-independent pathway. *J. Biol. Chem.* **269**, 3181–3188 (1994).
7. Spiegel, S., Cuvillier, O., Fuior, E. & Milstein, S. in *Sphingolipid-mediated Signal Transduction* (ed. Hannun, Y. A.) 121–135 (Springer, Berlin, 1997).
8. Pyne, S. & Pyne, N. J. Sphingosine 1-phosphate signalling in mammalian cells. *Biochem. J.* **349**, 385–402 (2000).
9. Merrill, A. H. Jr & Sweeley, C. C. in *Biochemistry of Lipids, Lipoproteins and Membranes* (eds Vance, D. E. & Vance, J.) 309–339 (Elsevier Science, Amsterdam, 1996).
10. Sullards, M. C., Lynch, D. V., Merrill, A. H. Jr & Adams, J. Structure determination of soybean and wheat glucosylceramides by tandem mass spectrometry. *J. Mass Spectrom.* **35**, 347–353 (2000).
11. Berger, A., Bittman, R., Schmidt, R. R. & Spiegel, S. Structural requirements of sphingosylphosphocholine and sphingosine-1-phosphate for stimulation of Activator Protein-1 activity. *Mol. Pharmacol.* **50**, 451–457 (1996).
12. McAinsh, M. R., Webb, A. A. R., Taylor, J. E. & Hetherington, A. M. Stimulus-induced oscillations in guard cell cytosolic free calcium. *Plant Cell* **7**, 1207–1219 (1995).
13. Gilroy, S., Read, N. D. & Trewavas, A. J. Elevation of cytoplasmic calcium by caged calcium or caged inositol trisphosphate initiates stomatal closure. *Nature* **346**, 769–771 (1990).
14. Blatt, M. R., Thiel, G. & Trentham, D. R. Reversible inactivation of K^+ channels of *Vicia* stomatal guard cells following the photolysis of caged inositol 1,4,5-trisphosphate. *Nature* **346**, 766–769 (1990).
15. Staxén, I. *et al.* Abscisic acid induces oscillations in guard-cell cytosolic calcium that involve phosphoinositide-specific phospholipase C. *Proc. Natl Acad. Sci. USA* **96**, 1779–1784 (1999).
16. Leckie, C. P., McAinsh, M. R., Allen, G. J., Sanders, D. & Hetherington, A. M. Abscisic acid-induced stomatal closure mediated by cyclic ADP-ribose. *Proc. Natl Acad. Sci. USA* **95**, 15837–15842 (1998).
17. McAinsh, M. R., Brownlee, C. & Hetherington, A. M. Abscisic acid-induced elevation of guard cell cytosolic Ca^{2+} precedes stomatal closure. *Nature* **343**, 186–188 (1990).
18. Schroeder, J. I. & Hagiwara, S. Repetitive increases in cytosolic Ca^{2+} of guard cells by abscisic acid activation of nonselective Ca^{2+} permeable channels. *Proc. Natl Acad. Sci. USA* **87**, 9305–9309 (1990).
19. Buehrer, B. M. & Bell, R. M. Inhibition of sphingosine kinase *in vitro* and in platelets. *J. Biol. Chem.* **267**, 3154–3159 (1992).
20. Kohama, T. *et al.* Molecular cloning and functional characterization of murine sphingosine kinase. *J. Biol. Chem.* **273**, 23722–23728 (1998).

Hedgehog acts as a somatic stem cell factor in the *Drosophila* ovary

Yan Zhang & Daniel Kalderon

Department of Biological Sciences, Columbia University, New York, New York 10027, USA

Secreted signalling molecules of the Hedgehog (Hh) family have many essential patterning roles during development of diverse organisms including *Drosophila* and humans[1,2]. Although Hedgehog proteins most commonly affect cell fate, they can also stimulate cell proliferation. In humans several distinctive cancers, including basal-cell carcinoma, result from mutations that aberrantly activate Hh signal transduction[3]. In *Drosophila*, Hh directly stimulates proliferation of ovarian somatic cells[4–6]. Here we show that Hh acts specifically on stem cells in the *Drosophila* ovary. These cells cannot proliferate as stem cells in the absence of Hh signalling, whereas excessive Hh signalling produces supernumerary stem cells. We deduce that Hh is a stem-cell factor and suggest that human cancers due to excessive Hh signalling might result from aberrant expansion of stem cell pools.

In adult *Drosophila* females, egg chambers are produced continuously in the germarium of each of the 15–18 ovarioles that are bundled together to form an ovary[7]. In regions 1 and 2a of the germarium, 16-cell germline cysts develop from germline stem cells (Fig. 1). Each cyst is enveloped by a monolayer of follicle cells in region 2b and separated from the next cyst by a short stalk as it buds from region 3 to form an egg chamber. Follicle and stalk cells derive from somatic stem cells that reside at the region 2a/2b border[8]. When a somatic stem cell divides, one daughter retains a stem cell identity and continues to divide as a stem cell for several days[8]. The other, 'pre-follicle cell' daughter proliferates for about eight cycles as its progeny associate with germline cysts, pass posteriorly down the ovariole over a 5–6-day period, and differentiate into multiple specialized cell types[7,8]. Hedgehog (Hh) is expressed selectively in specialized non-proliferating, somatic 'terminal filament' and 'cap' cells at the anterior tip of the germarium[4] (Fig. 1). Inactivation of Hh, using conditional *hh* alleles, arrests egg chamber budding, and causes germline cysts to accumulate in swollen germaria, suggesting that too few follicle cells are being produced[4]. Conversely, excessive Hh signalling in germarial region 2 can be induced by temporally controlled activation of an *hh* transgene or by inactivation of the Hh receptor Patched (Ptc), and causes marked overproliferation of somatic cells, which accumulate between egg chambers[4–6] (Fig. 2).

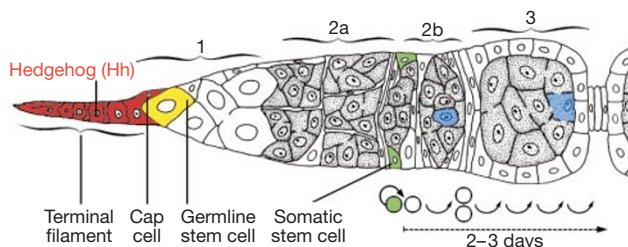We investigated the proliferative response to excessive Hh signal

Figure 1 The *Drosophila* germarium. Regions 1 and 2a contain large proliferating germline stem cells (yellow), cystoblasts and cystocyte clusters (shaded), and smaller non-proliferating somatic cells. Somatic stem cells (green) renew and produce pre-follicle daughter cells (colourless), which divide roughly five times in the germarium (∼50 h), three more times up to stage 6 (∼30 h) and then arrest before differentiation, and exit from the ovariole (∼30 h later). Hedgehog-producing cells and the oocyte are coloured red and blue respectively.

letters to nature

1. Berke, J. D. & Hyman, S. E. Addiction, dopamine, and the molecular mechanisms of memory. *Neuron* **25,** 515–532 (2000).
2. Nestler, E. J. Molecular mechanisms of opiate and cocaine addiction. *Curr. Opin. Neurobiol.* **7,** 713–719 (1997).
3. Hope, B. T. *et al.* Induction of a long-lasting AP-1 complex composed of altered Fos-like proteins in brain by chronic cocaine and other chronic treatments. *Neuron* **13,** 1235–1244 (1994).
4. Kelz, M. B. *et al.* Expression of the transcriptional factor ΔFosB in the brain controls sensitivity to cocaine. *Nature* **401,** 272–276 (1999).
5. Hiroi, N. *et al.* FosB mutant mice: Loss of chronic cocaine induction of Fos-related proteins and heightened sensitivity to cocaine's psychomotor and rewarding effects. *Proc. Natl Acad. Sci. USA* **94,** 10397–10402 (1997).
6. Chen, J. *et al.* Transgenic animals with inducible, targeted gene expression in the brain. *Mol. Pharmacol.* **54,** 495–503 (1998).
7. Bibb, J. A. *et al.* Phosphorylation of DARPP-32 by Cdk5 modulates dopamine signalling in neurons. *Nature* **402,** 669–671 (1999).
8. Snyder, G. L. *et al.* Phosphorylation of DARPP-32 and protein phosphatase inhibitor-1 in rat choroid plexus: Regulation by factors other than dopamine. *J. Neurosci.* **12,** 3071–3083 (1992).
9. Dulubova, I. *et al.* ARPP-16/ARPP-19: a highly conserved family of cAMP-regulated phosphoproteins. *J. Neurochem.* (in the press).
10. Caporaso, G. *et al.* Dopamine and drugs of abuse modulate phosphorylation of ARPP-21, a cyclic AMP-regulated phosphoprotein enriched in the neostriatum. *Neuropharmacology* **39,** 1637–1644 (2000).
11. Roche, K. W., O'Brien, R. J., Mammen, A. L., Bernhardt, J. & Huganir, R. L. Characterization of multiple phosphorylation sites on the AMPA receptor GluR1 subunit. *Neuron* **16,** 1179–1188 (1996).
12. White, F. J., Hu, X. -T., Zhang, X. -F. & Wolf, M. E. Repeated administration of cocaine or amphetamine alters neuronal responses to glutamate in the mesoaccumbens dopamine system. *J. Pharmacol. Exp. Ther.* **273,** 445–454 (1995).
13. Zhang, X. -F., Hu, X. -T. & White, F. J. Whole-cell plasticity in cocaine withdrawal: Reduced sodium currents in nucleus accumbens neurons. *J. Neurosci.* **18,** 488–498 (1998).
14. Dreher, J. K. & Jackson, D. M. Role of D1 and D2 dopamine receptors in mediating locomotor activity elicited from the nucleus accumbens of rats. *Brain Res.* **487,** 267–277 (1989).
15. Self, D. W., Barnhart, W. J., Lehman, D. A. & Nestler, E. J. Opposite modulation of cocaine-seeking behavior by D1- and D2-like dopamine receptor agonists. *Science* **271,** 1586–1589 (1996).
16. Xu, M. *et al.* Elimination of cocaine-induced hyperactivity and dopamine-mediated neurophysiological effects in dopamine D1 receptor mutant mice. *Cell* **79,** 945–955 (1994).
17. Nishi, A. *et al.* Amplification of dopaminergic signalling by a novel positive feedback loop. *Proc. Natl Acad. Sci. USA* **97,** 12840–12845 (2000).
18. Hiroi, N. *et al.* Neuronal and behavioural abnormalities in striatal function in DARPP-32-mutant mice. *Eur. J. Neurosci.* **11,** 1114–1118 (1999).
19. Chae, T. *et al.* Mice lacking p35, a neuronal specific activator of cdk5, displays cortical lamination defects, seizures, and adult lethality. *Neuron* **18,** 29–42 (1997).
20. Ohshima, T. *et al.* Targeted disruption of the cyclin-dependent kinase 5 gene results in abnormal corticogenesis, neuronal pathology and perinatal death. *Proc. Natl Acad. Sci. USA* **93,** 11173–11178 (1996).
21. Patrick, G. N. *et al.* Conversion of p35 to p25 deregulates Cdk5 activity and promotes neurodegeneration. *Nature* **402,** 615–622 (1999).
22. Zheng, M., Leung, C. L. & Liem, R. K. Region-specific expression of cyclin-dependent kinase 5 (cdk5) and its activators, p35 and p39, in the developing and adult rat central nervous system. *J. Neurobiol.* **35,** 141–159 (1998).
23. Le Moine, C. & Bloch, B. D1 and D2 dopamine receptor gene expression in the rat striatum: sensitive cRNA probes demonstrate prominent segregation of D1 and D2 mRNAs in distinct neuronal populations of the dorsal and ventral striatum. *J. Comp. Neurol.* **355,** 418–426 (1995).
24. Lee, H. -K., Kameyama, K., Huganir, R. L. & Bear, M. F. NMDA induces long-term synaptic depression and dephosphorylation of the GluR1 subunit of AMPA receptors in hippocampus. *Neuron* **21,** 1151–1162 (1998).
25. Ouimet, C. C. Immunocytochemical localization of protein phosphatases and their inhibitors. *Neuroprotocols* **6,** 84–90 (1995).
26. Horger, B. A. *et al.* Enhancement of locomotor activity and conditioned reward to cocaine by brain-derived neurotrophic factor. *J. Neurosci.* **19,** 4110–4122 (1999).
27. Taylor, J. R. & Horger, B. A. Enhanced responding for conditioned reward produced by intra-accumbens amphetamine is potentiated after cocaine sensitization. *Psychopharmacology* **142,** 31–40 (1999).
28. Punch, L., Self, D., Nestler, E. J. & Taylor, J. R. Opposite modulation of opiate withdrawal behaviors on microinfusion of a protein kinase A inhibitor versus activator into the locus coeruleus or periaquiductal gray. *J. Neurosci.* **17,** 8520–8527 (1997).
29. Surmeier, D. J., Bargas, J., Hemmings, H. C. Jr, Nairn, A. C. & Greengard, P. Modulation of calcium currents by a D1 dopaminergic protein kinase/phosphatase cascade in rat neostriatal neurons. *Neuron* **14,** 385–397 (1995).
30. Hamill, O. P., Marty, A., Neher, E., Sakmann, B. & Sigworth, F. J. Improved patch-clamp techniques for high resolution current recording from cells and cell-free membrane patches. *Pflüegers Arch.* **391,** 85–100 (1981).

Acknowledgements

BRI1 is a critical component of a plasma-membrane receptor for plant steroids

Zhi-Yong Wang*, Hideharu Seto†, Shozo Fujioka†, Shigeo Yoshida† & Joanne Chory*

*Howard Hughes Medical Institute and Plant Biology Laboratory, The Salk Institute for Biological Studies, 10010 N. Torrey Pines Road, La Jolla, California 92037, USA
† Plant Functions Lab, RIKEN (The Institute of Physical and Chemical Research), Wako-shi, Saitama 351-0198, Japan

Most multicellular organisms use steroids as signalling molecules for physiological and developmental regulation. Two different modes of steroid action have been described in animal systems: the well-studied gene regulation response mediated by nuclear receptors[1,2], and the rapid non-genomic responses mediated by proposed membrane-bound receptors[3,4]. Plant genomes do not seem to encode members of the nuclear receptor superfamily[5]. However, a transmembrane receptor kinase, brassinosteroid-insensitive1 (BRI1), has been implicated in brassinosteroid responses[6,7]. Here we show that BRI1 functions as a receptor of brassinolide, the most active brassinosteroid. The number of brassinolide-binding sites and the degree of response to brassinolide depend on the level of BRI1 protein. The brassinolide-binding activity co-immunoprecipitates with BRI1, and requires a functional BRI1 extracellular domain. Moreover, treatment of *Arabidopsis* seedlings with brassinolide induces autophosphorylation of BRI1, which, together with our binding studies, shows that BRI1 is a receptor kinase that transduces steroid signals across the plasma membrane.

Brassinosteroids (BRs) are involved in a wide range of plant developmental processes[8]. Mutant plants deficient in BR biosynthesis, such as *det2*, show phenotypes of dwarfism, delayed senescence, reduced fertility, and light-independent development[9,10]. Mutations in the *BRI1* gene cause BR-insensitivity and morphological phenotypes nearly identical to BR biosynthetic mutants, suggesting an important and specific role for *BRI1* in BR perception or signal transduction[11,12]. The *BRI1* gene encodes a receptor kinase that has an extracellular domain containing 25 leucine-rich repeats (LRRs), which are interrupted by a 70-amino-acid island, a transmembrane domain, and a cytoplasmic kinase domain with serine/threonine specificity[6,13]. The structure of BRI1 and its plasma membrane localization[13] support the hypothesis that BRI1 interacts with an extracellular ligand, which is either BR itself or a secondary signal generated by BR perception, and the signal is transduced through the kinase. Consistent with this hypothesis, recent studies using a chimaeric receptor approach showed that the extracellular domain of BRI1 could confer brassinolide (BL) responsiveness to the intracellular kinase domain of a heterologous LRR kinase[7].

To test whether BL is the ligand that directly activates the BRI1 receptor kinase, we first analysed the effect of overexpression of BRI1 on BL binding activity in membrane fractions. Transgenic *Arabidopsis* plants overexpressing a BRI1–GFP fusion protein[13] (GFP, green fluorescent protein) showed reduced inhibition of hypocotyl growth by a BR biosynthesis inhibitor[14] (Fig. 1a, b). They also had longer petioles, similar to plants overexpressing the BR biosynthetic enzyme DWF4[15] (Z.W. and J.C., unpublished data) (Fig. 1c). These phenotypes are consistent with the interpretation that overexpression of the BRI1–GFP protein increases the response of *Arabidopsis* to BRs. We observed a dramatic increase of BL binding activity in the membrane fractions of the BRI1–GFP transgenic plants (Fig. 1d). The increase of binding was due to an

increase of binding sites (maximum number of binding sites, $B_{max} = 2.66$ pmol per mg membrane protein compared to 0.23 pmol per mg membrane protein), with similar binding affinities (dissociation constant $K_d = 7.4 \pm 0.9$ nM compared to 10.8 ± 3.2 nM) (Fig. 1e). Such K_d values are consistent with physiological concentrations of BL[16,17] and coincide with the BL concentration that induces 50% of the maximum growth response in BL-deficient mutants[9].

We determined the specificity of the BL binding activity by comparing the relative binding affinity for several steroid compounds in binding competition assays (Fig. 1f). Binding of [3H]-BL to the membrane fraction of BRI1–GFP plants was effectively competed by unlabelled BL (50% inhibition concentration, IC_{50}, 80 nM), less effectively by castasterone (IC_{50}, 340 nM), and not competed by 2,3,22,23-O-tetramethylbrassinolide (Me-BL; $IC_{50} > 10\,\mu M$) and ecdysone ($IC_{50} > 10\,\mu M$). The relative binding affinity (the ratio between IC_{50} of a competitor and that of BL) of castasterone is about 4–5 times lower than BL, and this is consistent with castasterone being about 5 times less active than BL in bioassays[18]. The lack of competition by Me-BL and ecdysone is consistent with their lack of biological activity in
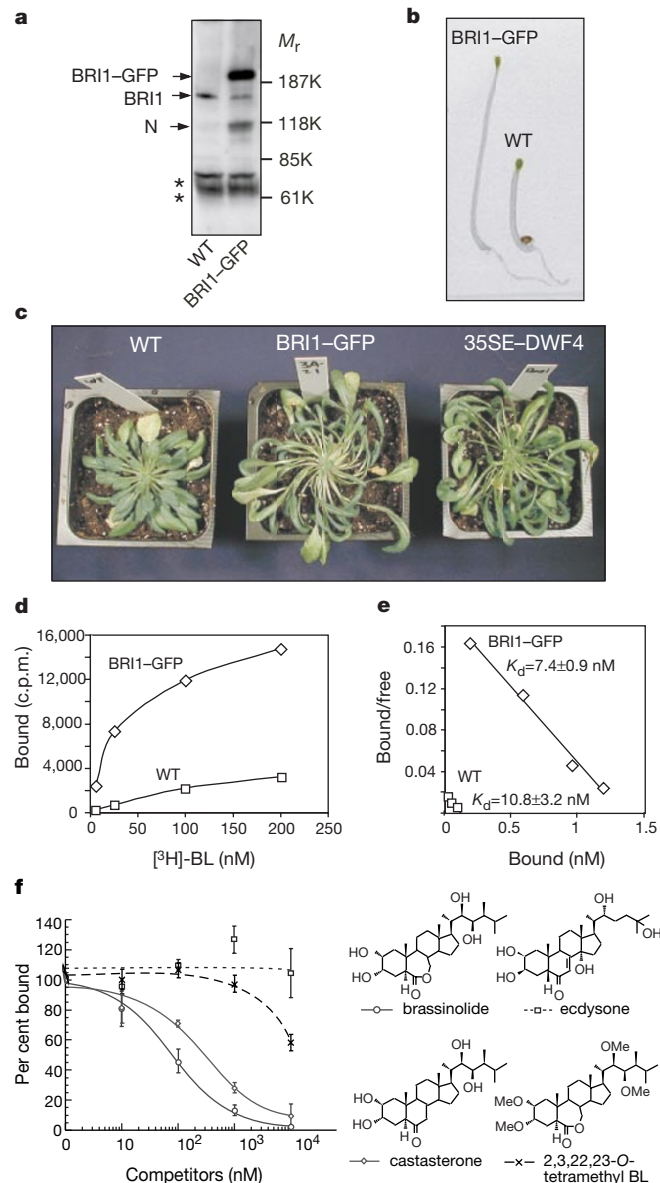

Figure 1 Overexpression of BRI1–GFP increases cell elongation and increases the number of brassinolide (BL) binding sites in membrane fractions. **a**, Proteins from wild-type and BRI1–GFP transgenic plants probed with anti-BRI1N antibody after western blotting. N, a cleaved fragment of BRI1's extracellular domain. Asterisks, non-specific bands. **b**, Wild-type (WT) and BRI1–GFP plants grown on $2\,\mu M$ brassinazole in the dark for 6 d. **c**, A wild-type plant, a BRI1–GFP transgenic plant, and a mutant plant overexpressing the *DWF4* gene (35SE-DWF4) grown for 45 d in cycles of 9 h light/15 h dark. **d**, Specific [3H]-BL binding to microsomal fractions of wild-type (WT) and BRI1–GFP plants was determined by subtracting the binding in the presence of 100-fold unlabelled BL from the total binding in the absence of cold competitor. Representative data of one of three repeat experiments are shown. **e**, Scatchard plot of the binding data in **d**. The K_d values were calculated from data of three experiments, with correlation coefficient $R^2 = 0.998$ for BRI1–GFP and 0.983 for wild-type samples. **f**, Competition for [3H]-BL binding to membrane fractions of BRI1–GFP plants by brassinolide, castasterone, ecdysone and 2,3,22,23-O-tetramethylbrassinolide. Structures of the competitors are shown.
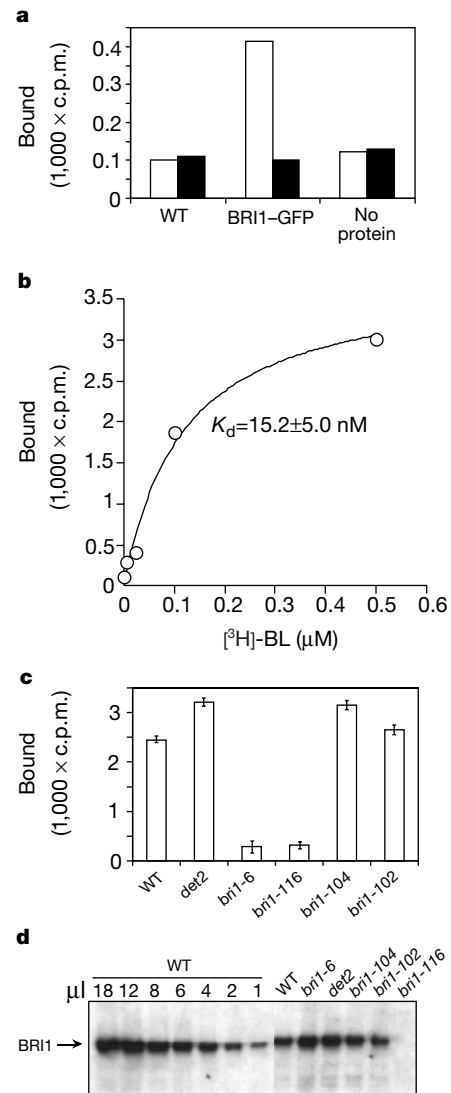

Figure 2 BRI1 binds to BL. **a**, Proteins immunoprecipitated with anti-GFP antibodies from extracts of wild-type or BRI1–GFP plants were assayed for [3H]-BL binding activity in the absence (open bars) or presence (filled bars) of $5\,\mu M$ unlabelled BL. No protein, binding assays with protein A beads as control. **b**, Specific and saturation [3H]-BL binding to immunoprecipitated BRI1–GFP protein. **c**, Mutations in the extracellular domain of BRI1, but not the kinase domain, reduce BL binding. Specific [3H]-BL binding to microsomal fractions of wild type (WT), *det2*, *bri1-6*, *bri1-116*, *bri1-104* and *bri1-102* mutant plants. Data were normalized to the relative BRI1 protein levels determined by quantitative western blotting (**d**), except for *bri1-116*. **d**, Protein immunoblot showing the BRI1 protein levels in the membrane fractions used in the binding assays of **c**. Varying loading of the wild-type sample was used to generate a standard curve, which was used to determine the relative level of BRI1 in the *bri1* mutant samples ($6\,\mu l$ per lane).

plants[19] (S.F., unpublished results). Such a specificity and high affinity for biologically active BRs indicate that this BL binding activity accounts for the BL-induced biological responses.

A specific BL binding activity was detected after the BRI1–GFP proteins were immunoprecipitated using anti-GFP antibodies (Fig. 2a, b). No specific BL binding activity was immunoprecipitated from wild-type *Arabidopsis* plants using the same antibodies (Fig. 2a), indicating that the BL binding activity is specific to the BRI1–GFP protein. The immunoprecipitated binding activity has a similar dissociation constant ($K_d = 15.2 \pm 5$ nM) as determined for membrane fractions (Fig. 2b). These results show that BRI1 either binds BL directly or is a limiting component of a receptor complex for BL in plant cells.

Mutations in large numbers of *bri1* alleles implicate the functional importance of the cytoplasmic kinase domain and the 70-amino-acid island of BRI1's extracellular domain[6,13,17]. We found that *bri1* mutants with missense mutations in the kinase domain (*bri1-104*, Ala1031Thr) or in a region of the extracellular domain near the transmembrane domain (*bri1-102*, Thr750Ile) have BL binding activities similar to wild type and the biosynthetic mutant *det2* (Fig. 2c, d). In contrast, a missense mutation (*bri1-6*, Gly644Asp) and a nonsense mutation that results in a truncated protein at position Gln 583 (*bri1-116*), both in the 70-amino-acid island region, greatly reduced the BL binding activity (Fig. 2c, d). These results provide direct evidence that the 70-amino-acid island region of BRI1's extracellular domain is required for BL binding to the receptor on the cell membrane.

We tested whether BL-binding activates BRI1's kinase. Receptor activation often involves auto-phosphorylation, which can lead to a

change of mobility in SDS–polyacrylamide gel electrophoresis (PAGE). *Arabidopsis* seedlings grown in the presence of the BR biosynthetic inhibitor brassinazole were treated with BL and analysed by immunoblotting (Fig. 3). Treatment of wild-type seedlings with 1 μM BL for 1 h caused a shift of BRI1 from a faster to a slower migrating band, compared with an untreated sample or a sample treated with mock solution (Fig. 3a). Phosphatase treatment of the BL-treated samples shifted the slower band back to the fast migrating band, suggesting that the shift of mobility represents BRI1 phosphorylation (Fig. 3b). We also observed such a BL-induced BRI1 mobility shift in the BL biosynthetic mutant *det2*, but not in the *bri1-117* mutant (Fig. 3c), which contains a mutation that abolishes BRI1's *in vitro* kinase activity (data not shown). Our data indicate that BL induction of BRI1 phosphorylation requires the kinase activity of BRI1, suggesting that BL-binding induces autophosphorylation of BRI1.

Our identification of the receptor kinase BRI1 as a plant steroid receptor illustrates the function of a member of the largest family of receptor kinases in *Arabidopsis*. The *Arabidopsis* genome sequence revealed 174 LRR-receptor kinases[5], of which only a few are known for their biological functions[20–22], and only one, CLV1, has been characterized at the biochemical level[20]. The mechanism by which BRI1 kinase is activated by ligand binding may be shared by other LRR-receptor kinases, as suggested by the BR activation of a BRI1-Xa21 chimaeric receptor[7]. However, BRI1 seems to differ from CLV1, which has recently been shown to require its own kinase activity for binding to its peptide ligand[20].

Our results also reveal a new mechanism of steroid signalling. Steroid hormones are generally known to pass freely across plasma membranes into animal cells, where they bind to members of the nuclear receptor superfamily of ligand-dependent transcription factors[1,2]. In contrast, the *Arabidopsis* genome does not seem to encode members of this family of proteins[5]. The near identical phenotypes of *bri1* to BR-biosynthetic mutants and our results presented here indicate that plants perceive steroids at the cell surface and that BRI1 is likely to be the primary BR receptor in *Arabidopsis*. A similar BL signalling mechanism is apparently conserved in other plants, as a homologue of BRI1 was shown recently to be required for BR responses in rice[23]. Such a cell-surface signalling mechanism may not be unique to plant steroids. In fact, membrane-initiated steroid responses have been observed in many animal systems, and signalling molecules such as calcium, inositol phosphates, cyclic AMP, G proteins and various kinases have been implicated[3]. However, little is known about the membrane-bound steroid receptors that initiate these signalling cascades in animal cells[4]. Considering the conservation of the steroid biosynthetic enzymes[24] and similar roles of steroids in growth and differentiation in plants and animals, it will be interesting to see if a similar membrane-based steroid signalling mechanism exists in both the animal and plant kingdoms. □
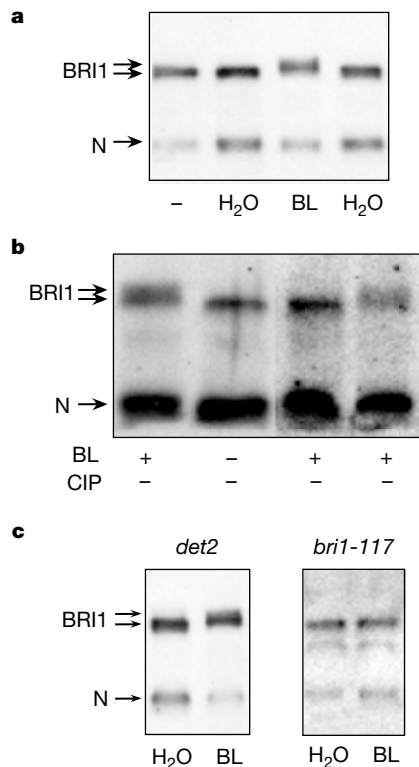
Methods

BL-binding assays

Tritium-labelled BL was made by American RadioChemicals using tritium reduction of 25,26-dehydrobrassinolide[25]. The specific activity of [³H]-BL was estimated to be 50 Ci mmol⁻¹, and the correct structure was confirmed by tritium NMR analysis. Biological activity of the [³H]-BL was determined by rescue of the *det2* mutant (data not shown). Plant microsomal fractions were prepared from *Arabidopsis* seedlings grown in a cycle of 9 h light/15 h dark for about 6 weeks, following a protocol described previously[7]. Membrane pellets were resuspended at a protein concentration of 2 mg ml⁻¹ in BL-binding buffer (0.25 M mannitol, 10 mM Tris-2-[N-morpholino] ethanesulphonic acid (MES), pH 5.7, 5 mM MgCl₂, 0.1 mM CaCl₂, and protease inhibitor cocktail (Sigma). Each BL binding assay contains 50 μl membrane suspensions, 50 nM or indicated amount of [³H]-BL, without or with 100-fold excess unlabelled BL or indicated amount of unlabelled steroids, 1 mg ml⁻¹ BSA and BL-binding buffer in 100 μl total volume. The binding reactions were incubated for 1 h or indicated time at 25 °C. The bound and free [³H]-BL were separated by filtering the mixture through a glass-fibre filter (Whatman, GF/F) and washing with 10 ml ice-cold BL-binding buffer, and were quantified by scintillation counting. Binding kinetic studies showed that the specific BL binding reaches equilibrium

Figure 3 BL induces phosphorylation of BRI1 in plants. **a**, Five-day-old wild-type seedlings grown in the dark on medium containing 1 μM brassinazole were untreated (–), treated with 1 μM BL in water (BL), or with water only (H₂O) for 1 h. Proteins were analysed by 4% SDS–PAGE, blotted, and probed with anti-BRI1N antibody. **b**, Proteins of the BL-treated wild-type sample were treated with alkaline phosphatase (CIP), and analysed by western blotting as in **a**. **c**, A mutation in the kinase domain abolishes BL-activation of BRI1 phosphorylation. The *det2* and *bri1-117* mutant seedlings were treated and analysed as in **a**. N, cleavage product of BRI1's extracellular domain.

within 15 min of incubation; the binding is highly reversible and 50% competition by unlabelled BL was achieved in less than 1 min (data not shown). For binding assays with immunoprecipitated proteins, proteins were extracted with BRI1 extraction buffer (2 ml per g tissue) (50 mM Tris-HCl, pH 7.5, 10 mM NaCl, 5 mM EDTA, 1% Triton X-100, and protease inhibitor cocktail), and GFP-tagged proteins were immunoprecipitated using anti-GFP antibodies (Molecular Probes, 1 µl per ml extract) and protein A agarose beads (10 µl per ml extract, Pierce). BL binding assays with immunoprecipitant/agarose beads were under the same conditions as for membrane fractions. Specific binding was determined by subtracting the binding in the presence of 100 fold unlabelled BL from total binding. Binding data were analysed and plotted using KaleidaGraph software (Synergy Software).

Immunoblotting and assays for BL-induced BRI1 phosphorylation

A peptide containing the first 106 amino acids of BRI1 (excluding the signal peptide) was expressed in *Escherichia coli* and purified as a maltose binding protein (MBP) fusion. This MBP–BRI1N fusion protein was used as an antigen for generating the anti-BRI1N antibodies in rabbits, and for affinity purification of the antibodies. The identities of the BRI1-containing bands detected by the anti-BRI1N antibodies on immunoblots were determined by comparing wild type, BRI1–GFP and *bri1-116* (a nonsense mutant) samples. To test BL induction of BRI1 phosphorylation, *Arabidopsis* seedlings were grown on MS medium plates containing 1 µM brassinazole in the dark for 4 d, submerged in water or in 1 µM BL solution for 1 min, then put back on MS plates without or with 1 µM BL for 1 h. Samples were analysed by SDS–PAGE using 4% gels and western blotting as described above[7]. For phosphatase treatment, SDS was removed from protein samples using the SDS-OUT kit (Pierce), and the proteins were then treated with alkaline phosphatase (Boehringer Mannheim) under conditions recommended by the manufacturer and described elsewhere[26].

1. Beato, M., Herrlich, P. & Schutz, G. Steroid hormone receptors: many actors in search of a plot. *Cell* **83**, 851–857 (1995).
2. Mangelsdorf, D. J. *et al.* The nuclear receptor superfamily: The second decade. *Cell* **83**, 835–839 (1995).
3. Wehling, M. Specific, nongenomic actions of steroid hormones. *Annu. Rev. Physiol.* **59**, 365–393 (1997).
4. Schmidt, B. M. *et al.* Rapid, nongenomic steroid actions: A new age? *Front. Neuroendocrinol.* **21**, 57–94 (2000).
5. The Arabidopsis Genome Initiative. Analysis of the genome sequence of the flowering plant *Arabidopsis thaliana. Nature* **408**, 796–815 (2000).
6. Li, J. & Chory, J. A putative leucine-rich repeat receptor kinase involved in brassinosteroid signal transduction. *Cell* **90**, 929–938 (1997).
7. He, Z. *et al.* Perception of brassinosteroids by the extracellular domain of the receptor kinase BRI1. *Science* **288**, 2360–2363 (2000).
8. Mandava, N. B. Plant growth-promoting brassinosteroids. *Annu. Rev. Plant Physiol. Plant Mol. Biol.* **39**, 23–52 (1988).
9. Li, J., Nagpal, P., Vitart, V., McMorris, T. C. & Chory, J. A role for brassinosteroids in light-dependent development of *Arabidopsis. Science* **272**, 398–401 (1996).
10. Wang, Z.-Y. & Chory, J. in *Recent Advances in Phytochemistry* Vol. 34, *Evolution of Metabolic Pathways* (eds Romeo, J. T., Ibrahim, R., Varin, L. & DeLuca, V.) 409–431 (Elsevier Science, Oxford, 2000).
11. Clouse, S. D., Langford, M. & McMorris, T. C. A brassinosteroid-insensitive mutant in *Arabidopsis thaliana* exhibits multiple defects in growth and development. *Plant Physiol.* **111**, 671–678 (1996).
12. Schumacher, K. & Chory, J. Brassinosteroid signal transduction: still casting the actors. *Curr. Opin. Plant Biol.* **3**, 79–84 (2000).
13. Friedrichsen, D. M., Joazeiro, C. A., Li, J., Hunter, T. & Chory, J. Brassinosteroid-insensitive-1 is a ubiquitously expressed leucine-rich repeat receptor Serine/Threonine kinase. *Plant Physiol.* **123**, 1247–1256 (2000).
14. Asami, T. *et al.* Characterization of brassinazole, a triazole-type brassinosteroid biosynthesis inhibitor. *Plant Physiol.* **123**, 93–100 (2000).
15. Choe, S. *et al.* The *DWF4* gene of *Arabidopsis* encodes a cytochrome P450 that mediates multiple 22alpha-hydroxylation steps in brassinosteroid biosynthesis. *Plant Cell* **10**, 231–243 (1998).
16. Clouse, S. & Sasse, J. Brassinosteroids: Essential regulators of plant growth and development. *Annu. Rev. Plant Physiol. Plant Mol. Biol.* **49**, 427–451 (1998).
17. Noguchi, T. *et al.* Brassinosteroid-insensitive dwarf mutants of *Arabidopsis* accumulate brassinosteroids. *Plant Physiol* **121**, 743–752 (1999).
18. Fujioka, S., Noguchib, T., Takatsutod, S. & Yoshida, S. Activity of brassinosteroids in the dwarf rice lamina inclination bioassay. *Phytochemistry* **49**, 1841–1848 (1998).
19. Luo, W., Janzen, L., Pharis, R. P. & Back, T. G. Bioactivity of brassinolide methyl ethers. *Phytochemistry* **49**, 637–642 (1998).
20. Trotochaud, A. E., Jeong, S. & Clark, S. E. CLAVATA3, a multimeric ligand for the CLAVATA1 receptor-kinase. *Science* **289**, 613–617 (2000).
21. Torii, K. U. *et al.* The *Arabidopsis ERECTA* gene encodes a putative receptor protein kinase with extracellular leucine-rich repeats. *Plant Cell* **8**, 735–746 (1996).
22. Jinn, T. L., Stone, J. M. & Walker, J. C. HAESA, an Arabidopsis leucine-rich repeat receptor kinase, controls floral organ abscission. *Genes Dev.* **14**, 108–117 (2000).
23. Yamamuro, C. *et al.* Loss of function of a rice *brassinosteroid insensitive1* homolog prevents internode elongation and bending of the lamina joint. *Plant Cell* **12**, 1591–1605 (2000).
24. Li, J., Biswas, M. G., Chao, A., Russell, D. W. & Chory, J. Conservation of function between mammalian and plant steroid 5alpha- reductases. *Proc. Natl Acad. Sci. USA* **94**, 3554–3559 (1997).
25. Seto, H. *et al.* A general approach to synthesis of labeled brassinosteroids: preparation of [25,26,27-²H₇]brassinolide with 60% isotopic purity from the parent brassinolide. *Tetrahedr. Lett.* **39**, 7525–7528 (1998).
26. Fankhauser, C. *et al.* PKS1, a substrate phosphorylated by phytochrome that modulates light signaling in *Arabidopsis. Science* **284**, 1539–1541 (1999).

....

Regulation of CD40 and CD40 ligand by the AT-hook transcription factor AKNA

Aisha Siddiqa*†, **Jennifer C. Sims-Mourtada***†, **Liliana Guzman-Rojas***†, **Roberto Rangel***†, **Christiane Guret**‡, **Vicente Madrid-Marina**§, **Yan Sun**† & **Hector Martinez-Valdez**†

† *Department of Immunology, Box 178, The University of Texas M. D. Anderson Cancer Center, 1515 Holcombe Boulevard, Houston, Texas 77030, USA*
‡ *Laboratory for Immunology Research, Schering-Plough, 27 Chemin des Peupliers, 69571 Dardilly, Cedex, France*
§ *Centro de Investigacion Sobre Enfermedades Infecciosas, Instituto Nacional de Salud Publica, Ave. Universidad 655, Cuernavaca, Morelos, 62508, Mexico*
* *These authors contributed equally to this work.*

....

Proteins containing AT hooks bind A/T-rich DNA through a nine-amino-acid motif and are thought to co-regulate transcription by modifying the architecture of DNA, thereby enhancing the accessibility of promoters to transcription factors[1,2]. Here we describe AKNA, a human AT-hook protein that directly binds the A/T-rich regulatory elements of the promoters of CD40 and CD40 ligand (CD40L) and coordinately regulates their expression. Consistent with its function, AKNA is a nuclear protein that contains multiple PEST protein-cleavage motifs, which are common in regulatory proteins with high turnover rates[3]. AKNA is mainly expressed by B and T lymphocytes, natural killer cells and dendritic cells. During B-lymphocyte differentiation, AKNA is mainly expressed by germinal centre B lymphocytes, a stage in which receptor and ligand interactions are crucial for B-lymphocyte maturation[4–12]. Our findings show that an AT-hook molecule can coordinately regulate the expression of a key receptor and its ligand, and point towards a molecular mechanism that explains homotypic cell interactions.

Earlier studies of lymphocyte maturation indicated the possible existence of stage-specific molecules that could regulate ligand and receptor gene expression[12–15]. To test this hypothesis, we performed a polymerase chain reaction with reverse transcriptase (RT–PCR) differential display[16], using RNA from pure human B-lymphocyte subsets[9]. PCR products were purified, cloned, sequenced and compared against gene databases[17], revealing that seven of the twelve PCR clones were known genes. AKNA and another protein, PRELI[18], were differentially expressed by germinal centre B lymphocytes and were among the five new complementary DNAs.

Northern blotting revealed a 4-kilobase (kb) AKNA messenger RNA predominantly expressed by lymphoid tissues (Fig. 1). The expression was highest in the spleen, lymph nodes and peripheral